QUARK–GLUON PLASMA IN PB–PB 158 *A* GEV COLLISIONS: EVIDENCE FROM STRANGE PARTICLE ABUNDANCES AND THE COULOMB EFFECT

Jean Letessier and Jan Rafelski

Laboratoire de Physique Théorique et Hautes Energies
Université Paris 7, 2 place Jussieu, F–75251 Cedex 05
Department of Physics, University of Arizona, Tucson, AZ 85721

(Received October 21, 1998)

The hadronic particle production data from relativistic nuclear Pb–Pb 158 *A* GeV collisions are successfully described within the chemical non-equilibrium model, provided that the analysis treats Ω and $\overline{\Omega}$ abundances with care. We further show that there is a subtle influence of the Coulomb potential on strange quarks in quark matter which is also seen in our data analysis, and this Coulomb effect confirms the finding made by chemical analysis in the S–Au/W/Pb 200 *A* GeV collisions that the hadron particle source is deconfined with respect to strange quark propagation. Physical freeze-out conditions (pressure, specific energy, entropy, and strangeness) are evaluated and considerable universality of hadron freeze-out between the two different collision systems is established.

PACS numbers: 25.75.-q, 12.38.Mh, 24.85.+p

1. Introduction

Intense experimental and theoretical work proceeds to explore the mechanisms of quark confinement effect and the properties of the vacuum state of quantum-chromodynamics (QCD), the non-Abelian gauge theory of 'color' charges [1]. Relativistic energy nuclear collisions are the novel experimental tool developed in the past decade to form, study, and explore the 'melted' space-time domain, where we hope to find, beyond the Hagedorn temperature $T_{\rm H} \simeq 160$ MeV [2], freely propagating quarks and gluons in the (color charge) plasma (QGP). Analysis of hadronic particle production in relativistic nuclear collisions offers an opportunity to explore the mechanisms of quark confinement at the time of final state QGP freeze-out. We present here a progress report of such ongoing analysis of the recent experimental

results regarding the Pb–Pb collisions at 158 A GeV [3], which follows on our now complete analysis of the S–Au/W/Pb collision systems [4].

There is little doubt that in the early Universe QGP was the transient state of matter, and that only about 20–40 μsec into evolution did our present confining vacuum freeze-out from the primordial QGP-form. The issue is if in laboratory experiments we can indeed form and study the primordial QGP phase [5]. In some aspects, such as specific entropy and baryon content, notable differences between the laboratory QGP state and the early Universe conditions are present. Also, the small, nuclear size of the nuclear collision 'micro'-bang implies a short laboratory lifespan $\tau_q \simeq 0.5 \cdot 10^{-22}$sec. There is also the difficult problem of proving the fundamental paradigm beyond a shade of doubt: can there indeed exist a locally deconfined space-time domain with energy density exceeding by an order of magnitude that of nuclear matter? Much of the current effort is solely addressing this question. Among several proposed approaches to search for and study the deconfinement, our work relies on the idea of strangeness flavor enhancement, and the associated enhancement of (strange) antibaryon formation [6]. This signature can be combined, in the present analysis, with the study of global particle abundance which represents the entropy contents of the deconfined phase [7, 8].

We address here 15 presently available particle yield ratios obtained in central Pb–Pb 158 A GeV collision experiments carried out at CERN-SPS. Our analysis addresses results of experiments NA49 [9, 10], and WA97 [11], we have not used results from NA44 [12], being uncertain about the impact of the cascading weak decay contamination of the hadronic ratios, which are quite significant. Four WA97 data points involve Ω and $\overline{\Omega}$ particles and even a cursory study of these abundances suggests that these entirely strange particles are not falling into the same systematic class, a fact also visible in their unusual spectral slopes. We believe in view of the difference in systematics that it is appropriate also to consider the data excluding the Ω and $\overline{\Omega}$ yields from analysis. In that case our analysis contains 11 relative experimental particle yields. However, 4 of these ratios originating in the same experiment are related by a simple algebraic constraint (*e.g.,* $\overline{\Lambda}/\Lambda = \overline{\Lambda}/\overline{\Xi} \cdot \overline{\Xi}/\Xi \cdot \Xi/\Lambda$), leaving us with ten independent measurements. As we shall see, there are up to 5 parameters in our description. In the different analysis discussed here we thus have no less than 5 independent degrees of freedom: $n_{\rm dof} \geq 5$. Since we address ratios of strange particles as well as ratios of total abundances of positive and negative hadrons, we combine in the present analysis strangeness observables with the entropy enhancement [7]. Underlying our data analysis is the assumption of local thermal (*i.e.,* energy equipartition) equilibrium. Both, the thermal appearance of produced particle spectra [2,4,13], and the qualitative and systematic agreement over many orders of magni-

tude between properties of a thermal hadron system and the experimental hadron abundance yields [14], provide a solid foundation for the assumption of (near) thermal equilibrium in the dense hadronic matter.

In our most recent theoretical approach there is a key refinement not present in earlier work [4]: we do not assume chemical equilibrium even for light quarks. Consideration of non-equilibrium chemical abundance for strange quarks allowed to analyze accurately the experimental particle abundance data and to characterize precisely the properties of the presumably deconfined source [3,7,10,12,15,16,17,18,19,20]. The mechanisms of chemical equilibration requiring reactions which change particle abundances are today much better understood theoretically than those responsible for what is believed to be much faster thermal (kinetic) equilibration, where momentum exchange between existent particles is the key mechanism. It is hard to understand, why we, along with others, have maintained in the past in our analysis the point of view that only strangeness has the opportunity to be off-equilibrium in chemical abundance. Indeed, if QGP is the particle source the need to assimilate by fragmentation the gluon content must generate excess light quark abundance. Since we did not allow for this freedom in earlier data analysis, the data were (equally badly) also described by a high temperature source model [3]. This is not the case once also for light quarks the chemical nonequilibrium is introduced, only the low temperature freeze-out alternative has a convincing statistical significance

Hadronic particles we observe are either emitted directly or are descendants of other hadronic primaries produced near or at surface of the dense matter fireball. Local rest-frame temperature T and local collective flow velocity $\vec{v}_{\rm c}$ characterize the momentum space distribution of particles emerging from the surface region of the fireball. In addition, each surface volume element is characterized by chemical abundance factors we shall discuss in more detail below. Only particles of similar mass and cross section experience similar drag forces arising from local flow of matter and hence ratio of their abundances in some limited region of phase space for not too small momenta is expected to remain unaltered by $\vec{v}_{\rm c}$. Since the surface vector flow $\vec{v}_{\rm c}$ is a priori largely unknown, in order to use limited 'windows' of particle momenta (rapidity y and transverse mass $m_\perp$) for determination of chemical freeze-out properties of the source, only ratios of 'mutually compatible' particles can be considered, aside of ratios of total particle abundances. Our recent study of the flow effect shows that this procedure is adequate, though with the ongoing improvement of the data sample we will soon have to include this additional freeze-out flow velocity parameter explicitly in the analysis [21].

In the following Section, we shall briefly summarize the theoretical foundations of the current analysis and discuss the impact of Coulomb effect in

QGP on the expected values of statistical parameters, and we shall describe the parameters that we obtain. In Section 3, we will discuss the particle abundances and other related results, such as the physical properties of the freeze-out dense matter. We conclude with a few brief remarks about the relevance of our analysis for the search for QGP.

2. Statistical model and Coulomb effect

The thermal production yield dN_i of particles emitted within the time dt from a locally at rest surface element dS is:

$$dN_i = \frac{dSd^3p}{(2\pi)^3} A_i v_i dt\,. \tag{1}$$

Here $v_i = dz/dt$ is the particle velocity normal to the surface element $dS = dx\,dy$. For a thermal quark-gluon gas source and allowing for recombination-fragmentation of constituents and detailed balance, the complete phase space occupancy factor A_i is given by:

$$A_i = g_i\lambda_i\gamma_i \mathrm{e}^{-E_i/T}\,, \qquad \lambda_i = \prod_{j\in i}\lambda_j\,, \quad \gamma_i = \prod_{j\in i}\gamma_j\,, \quad E_i = \sum_{j\in i} E_j\,, \tag{2}$$

where g_i is the degeneracy of the produced particle, and E_i its energy. The valance quark content $\{j\}$ in hadron $\{i\}$ is implied in Eq. (2). The fugacities λ_j arise from conservation laws, in our context, of quark (baryon) number and strangeness in the particle source. $\lambda_q \equiv \mathrm{e}^{\mu_q/T}$ is thus the fugacity of the valance light quarks. For a nucleon $\lambda_N = \lambda_q^3$, and hence the baryochemical potential is: $\mu_b = 3\mu_q$. Similarly, for strange quarks we have $\lambda_s \equiv \mathrm{e}^{\mu_s/T}$. For an antiparticle fugacity $\lambda_{\bar{i}} = \lambda_i^{-1}$. Some papers refer in this context to hyper-charge fugacity $\lambda_{\mathrm{S}} = \lambda_q/\lambda_s$, thus $\mu_{\mathrm{S}} = \mu_q - \mu_s$. This is a highly inconvenient historical definition arising from considerations of a hypothetical hadron gas phase. It hides from view important symmetries, such as $\lambda_s \to 1$ for a state in which the phase space size for strange and anti-strange quarks is the same: at finite baryon density the number of hyperons is always greater than the number of anti-hyperons and thus the requirement $\langle N_s - N_{\bar{s}}\rangle = 0$ can only be satisfied for some nontrivial $\lambda_s(\lambda_q) \neq 1$. Thus even a small deviation from $\lambda_s \to 1$ limit must be fully understood in order to argue that the source is deconfined. Conversely, observation of $\lambda_s \simeq 1$ consistently at different experimental conditions is a strong and convincing argument that at least the strange quarks are unbound, *i.e.,* deconfined.

As this discussion also illustrates, the parameter λ_s does not regulate the total number of s-$\bar{s}$ quark-pairs present in the system. More generally, any compound object comprising a particle-antiparticle pair is not controlled in

abundance by a fugacity, since the formation of such particles does not impact the conservation laws. In consequence, the abundance of, *e.g.,* neutral pions comprises no quark fugacity. This is the reason to introduce an additional chemical phase space occupancy factor γ_i: the effective fugacity of quarks is $\lambda_i\gamma_i$ and antiquarks $\lambda_i^{-1}\gamma_i$. This parameter allows to control pair abundance independently of other properties of the system, and in particular temperature. For $\gamma_i \to 1$ one reaches a entropy maximum [8], corresponding to the 'absolute' chemical equilibrium [22]. Therefore the factor γ_i is called the (chemical) phase space occupancy factor.

A time dependent build up of chemical abundance was first considered in the context of microscopic strangeness production in QGP [22,23], after it was realized that strange flavor production occurs at the same time scale as the collision process. More generally, one must expect, considering the time scales, that all quark flavors will not be able to exactly follow the rapid evolution in time of dense hadronic matter. Moreover, fragmentation of gluons in hadronizing QGP can contribute additional quark pair abundance, conveniently described by the factor γ_i. It is thus to be expected that also for light quarks the chemical phase space occupancy factor $\gamma_q \neq 1$. Introduction of the factor γ_q leads to a precise chemical description of the S–Au/W/Pb 200 A GeV collisions [4], which was not possible before. The tacit choice $\gamma_q = 1$ has not allowed previously to distinguish the different reaction scenarios in Pb–Pb collisions [3], where we found analyzing the experimental data that hadronic particles could be born either at high temperature $T \simeq 300\,\mathrm{MeV}$ or at expected hadronization temperature $T \simeq 150\,\mathrm{MeV}$. Introduction of γ_q, along with improvement in precision, allowance for quantum (Bose/Fermi) corrections to the Boltzmann distribution functions, and a greater data sample, allowed us moreover to recognize the systematic difference between data points containing, and resp., not containing Ω, $\overline{\Omega}$, allowing us to develop the precise analysis here presented.

In another refinement both u, d-flavor fugacities λ_u and λ_d can be introduced, allowing for up-down-quark asymmetry [7]. We recall that by definition $2\mu_q = \mu_d + \mu_u$, thus $\lambda_q \equiv \sqrt{\lambda_u\lambda_d}$. For the highly Coulomb-charged fireballs formed in Pb–Pb collisions a further effect of the same relative magnitude which needs consideration is the distortion of the particle phase space by the Coulomb potential. This effect influences particles and antiparticles in opposite way, and has by factor two different strength for u-quark (charge $+2/3|e|$) and (d,s)-quarks (charge $-1/3|e|$). Because Coulomb-effect acts in opposite way on u and d quarks, its net impact on λ_q is relatively small as we shall see.

However, the Coulomb effect distorts significantly the expectation regarding $\lambda_s \to 1$ for strangeness-deconfined source with vanishing net strangeness. The difference between strange and anti-strange quark numbers (net

strangeness) allowing for a Coulomb potential within a relativistic Thomas–Fermi phase space occupancy model [24], allowing for finite temperature in QGP is

$$\langle N_s - N_{\bar{s}} \rangle = \int\limits_{R_\mathrm{f}} g_s \frac{d^3r d^3p}{(2\pi)^3} \left[\frac{1}{1+\gamma_s^{-1}\lambda_s^{-1}\mathrm{e}^{(E(p)-\frac{1}{3}V(r))/T}} - \frac{1}{1+\gamma_s^{-1}\lambda_s \mathrm{e}^{(E(p)+\frac{1}{3}V(r))/T}} \right], \tag{3}$$

which clearly cannot vanish for $V \neq 0$ in the limit $\lambda_s \to 1$. In Eq. (3) the subscript R_f on the spatial integral reminds us that only the classically allowed region within the fireball is covered in the integration over the level density; $E = \sqrt{m^2+\vec{p}^2}$, and for a uniform charge distribution within a radius R_f of charge Z_f:

$$V = \begin{cases} -\frac{3}{2}\frac{Z_\mathrm{f}e^2}{R_\mathrm{f}} \left[1 - \frac{1}{3}\left(\frac{r}{R_\mathrm{f}}\right)^2\right], & \text{for} \quad r < R_\mathrm{f}\,; \\ -\frac{Z_\mathrm{f}e^2}{r}, & \text{for} \quad r > R_\mathrm{f}\,. \end{cases} \tag{4}$$

One obtains a rather precise result for the range of parameters of interest to us (see below) using the Boltzmann approximation:

$$\langle N_s - N_{\bar{s}} \rangle = \gamma_s \left\{ \int g_s \frac{d^3p}{(2\pi)^3} \mathrm{e}^{-E/T} \right\} \int\limits_{R_\mathrm{f}} d^3r \left[\lambda_s \mathrm{e}^{\frac{V}{3T}} - \lambda_s^{-1} \mathrm{e}^{-\frac{V}{3T}} \right]. \tag{5}$$

The Boltzmann limit allows also to verify the signs: the Coulomb potential is negative for the negatively charged s-quarks with the magnitude of the charge, 1/3, made explicit in the potential terms in all expressions above. It turns out that there is always only one solution, with resulting $\lambda_s > 1$. The magnitude of the effect is quite significant: choosing $R_\mathrm{f} = 8\,\mathrm{fm}$, $T = 140\,\mathrm{MeV}$, $m_s = 200\,\mathrm{MeV}$ (value of $0.5 < \gamma_s < 2$ is irrelevant) solution of Eq. (3) for $Z_\mathrm{f} = 150$ yields $\lambda_s = 1.10$ (precisely: 1.0983, 1.10 corresponds to $R_\mathrm{f} = 7.87\,\mathrm{fm}$). This result is consistent with one of the scenarios we reported earlier for Pb–Pb collisions [3]. Thus we are reassured that the experimental data is very likely consistent with deconfined quark source, and hence a detailed verification of this hypothesis is needed. The remarkable result we find is that experimental data is only consistent with this value $\lambda_s = 1.10 \pm 0.02$, see Table I.

TABLE I

Statistical parameters obtained seeking minimum of weighted least square difference with experimental results shown in Table II. Values of $\lambda_{\rm s}$ in approach $\rm D_{\it s}$ is the result of strangeness conservation constraint: asterisk * means a fixed (input) value, not a parameter. In case $\rm D_{\it t}$ the temperature is fixed at the value obtained for S–Au/W/Pb collisions, and in case $\rm D_{\it p}$, the pressure in the hadronic phase space is fixed at 82 ± 6 MeV/fm^3, the value obtained in S–Au/W/Pb collisions. In case F the four ratios with Ω-data are studied.

Fit	$T_{\rm f}$ [MeV]	$\lambda_{\rm q}$	$\lambda_{\rm s}$	$\gamma_{\rm s}$	$\gamma_{\rm q}$	$n_{\rm dof}$	$\chi^2/n_{\rm dof}$
A	147 ± 3	1.69 ± 0.03	1^*	1^*	1^*	8	16
B	142 ± 3	1.70 ± 0.03	1.10 ± 0.02	1^*	1^*	7	13
C	144 ± 4	1.62 ± 0.03	1.10 ± 0.02	0.63 ± 0.04	1^*	6	4
D	134 ± 3	1.62 ± 0.03	1.10 ± 0.02	1.27 ± 0.08	1.84 ± 0.30	5	0.3
$\rm D_{\it s}$	133 ± 3	1.63 ± 0.03	$1.09^* \pm 0.02$	1.98 ± 0.12	2.75 ± 0.35	5	0.45
$\rm D_{\it t}$	143^*	1.61 ± 0.03	1.10 ± 0.02	0.74 ± 0.06	1.15 ± 0.18	5	0.8
$\rm D_{\it p}$	137 ± 4	1.62 ± 0.03	1.10 ± 0.02	0.88 ± 0.07	1.33 ± 0.10	5	0.5
F	334 ± 18	1.61 ± 0.03	1.12 ± 0.02	0.09 ± 0.01	0.18 ± 0.02	8	2.4

Thus as before for the lighter system S–Au/W/Pb [7, 15, 4] we are finding that the source of strange hadrons (up to Coulomb-asymmetry) is governed by a symmetric, and thus presumably deconfined strange quark phase space.

Let us briefly explain how we obtain the statistical parameters shown in Table I: with $E_i = \sqrt{m_i^2 + p^2} = \sqrt{m_i^2 + p_\perp^2}\cosh y$ we integrate over the transverse momentum range as given by the experiment, see Table II. To obtain the relative strengths of centrally produced particles we consider only central rapidity region $y \simeq 0$. We allow all hadronic resonances to disintegrate in order to obtain the final relative multiplicity of 'stable' particles required to form the observed particle ratios. We show results of four main models denoted A, B, C, D in top section of Table I, arising describing the data shown in the first 4 columns of Table II. In this group we successively relax the chemical variables from their tacit values (= 1). In each step the number of degrees of freedom decreases by one, yet as described by $\chi^2/n_{\rm dof}$ the confidence level becomes progressively better, and is indeed of impressive quality, with $\chi^2/n_{\rm dof} = 0.3$ when all 4 chemical variables are allowed to vary. We thus conclude that it is necessary in description of the particle abundance data to allow non-equilibrium abundances of light and strange quarks.

This is confirmed by the results we show in Fig. 1, where for a given $T_{\rm f}$, for case D (solid line, no Ω or strangeness conservation) and case $\rm D_s$ (dashed line, no Ω, with strangeness conservation), with all the other parameters obtained finding minimum of weighted least square theory-experiment difference at given temperature. The locations of the best $\chi^2/n_{\rm dof}$ are indicated by vertical lines. The top sections of the figure shows that both chemical non-equilibrium parameters $\gamma_{\rm s}$, $\gamma_{\rm q} > 1$ in a wide range of freeze-out temperatures, indeed the values are slightly higher for the smaller $T_{\rm f}$ that are normally more favored on intuitive grounds (lower freeze-out particle density). However, freeze-out at $T_{\rm f} > 145\,{\rm MeV}$ would allow values $\gamma_{\rm s}$, $\gamma_{\rm q} < 1$. It is reassuring that the analysis with matter flow [21] even more clearly favors the high values of $\gamma_{\rm s}$, $\gamma_{\rm q} > 1$ we found here. We note also the constancy of the parameter $\lambda_{\rm s}$ (unconstrained solid line result) which assures us that the Coulomb effect we described cannot be ignored. We also note the counter-intuitive result that the energy per baryon at freeze-out obtained from the properties of the hadronic phase space using the statistical parameters, is dropping as the freeze-out temperature increases in the region of interest here.

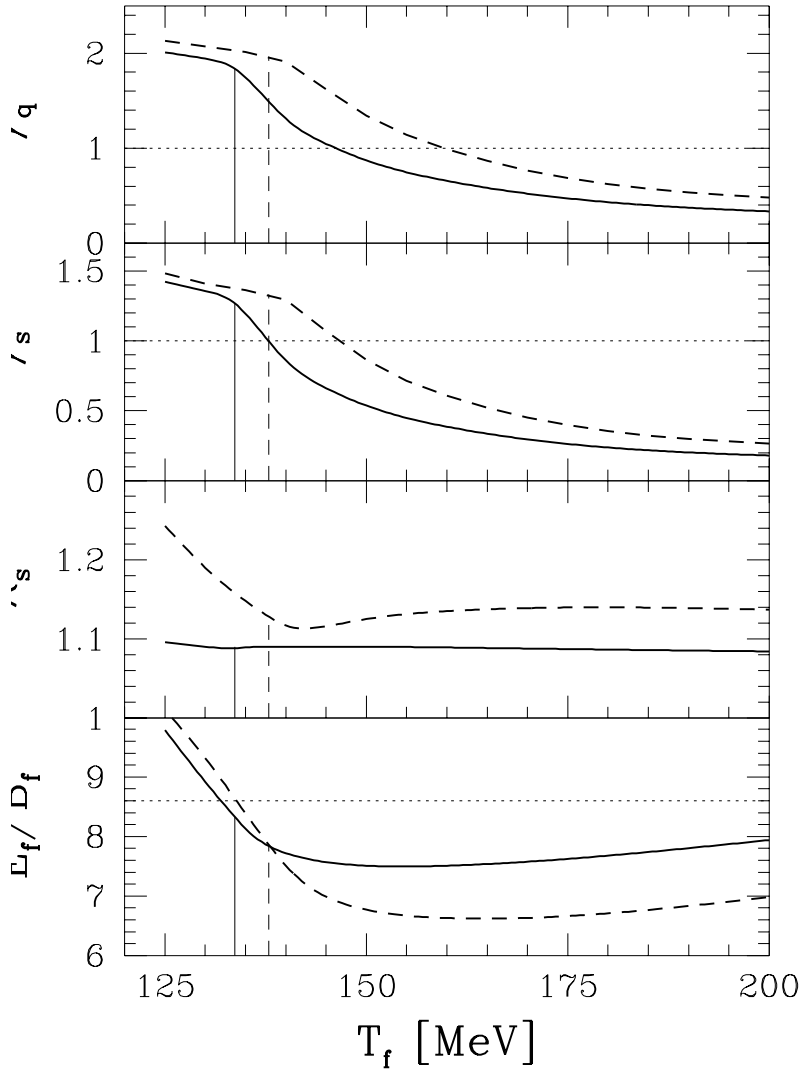

Fig. 1. Variation of γ_q, γ_s, λ_s, and E_f/B_f, as function of temperature T_f, with all other parameters fixed by choosing best agreement with the experimental data.

TABLE II

Particle ratios: Experimental results for Pb–Pb, references and kinematic domain in first four columns, and different model results corresponding to those shown in Table I in the remaining columns; Asterisk * means the corresponding experimental result is not fitted.

Ratio	Ref.	cuts[GeV]	Exp. data	Fit A	Fit B	Fit C	Fit D	Fit D_s	Fit D_t	Fit D_p	Fit F
Ξ/Λ	[11]	$p_\perp > 0.7$	0.099 ± 0.008	0.130	0.138	0.093	0.095	0.098	0.095	0.093	0.107
$\overline{\Xi}/\bar{\Lambda}$	[11]	$p_\perp > 0.7$	0.203 ± 0.024	0.361	0.322	0.198	0.206	0.215	0.201	0.201	0.216
$\bar{\Lambda}/\Lambda$	[11]	$p_\perp > 0.7$	0.124 ± 0.013	0.126	0.100	0.121	0.120	0.119	0.123	0.120	0.121
$\overline{\Xi}/\Xi$	[11]	$p_\perp > 0.7$	0.255 ± 0.025	0.351	0.232	0.258	0.260	0.263	0.262	0.258	0.246
$\frac{(\Xi+\bar{\Xi})}{(\Lambda+\bar{\Lambda})}$	[9]	$p_\perp > 1.$	0.13 ± 0.03	0.169	0.169	0.114	0.118	0.122	0.116	0.115	0.120
K^0_s/ϕ	[9]		11.9 ± 1.5	6.42	6.3	10.4	9.89	9.69	10.1	10.2	16.1
K^+/K^-	[9]		1.80 ± 0.10	2.27	1.96	1.75	1.76	1.73	1.73	1.77	1.62
$p/\bar{p}$	[9]		$18.1 \pm 4.$	20.5	22.0	17.1	17.3	17.9	16.6	17.3	16.7
$\bar{\Lambda}/\bar{p}$	[9]		$3. \pm 1.$	2.97	3.02	2.91	2.68	3.45	2.91	2.96	0.65
K^0_s/B	[9]		0.183 ± 0.027	0.298	0.305	0.224	0.194	0.167	0.211	0.214	0.242
h^-/B	[9]		1.83 ± 0.2	1.30	1.47	1.59	1.80	1.86	1.55	1.72	1.27
Ω/Ξ	[11]	$p_\perp > 0.7$	0.192 ± 0.024	0.115*	0.119*	0.080*	0.078*	0.080*	0.082*	0.078*	0.192
$\overline{\Omega}/\overline{\Xi}$	[11]	$p_\perp > 0.7$	0.27 ± 0.06	0.32*	0.28*	0.17*	0.17*	0.18*	0.18*	0.17*	0.40
$\overline{\Omega}/\Omega$	[11]	$p_\perp > 0.7$	0.38 ± 0.10	1.00*	0.55*	0.56*	0.57*	0.59*	0.56*	0.56*	0.51
$\frac{(\Omega+\overline{\Omega})}{(\Xi+\bar{\Xi})}$	[11]	$p_\perp > 0.7$	0.20 ± 0.03	0.17*	0.15*	0.10*	0.10*	0.10*	0.10*	0.10*	0.23

3. Hadronic particle abundances and phase space properties

Since we have the statistical parameters in hand, we can as alluded to above, not only obtain the particle abundances within the kinematic cuts, shown in Table II, but also study the physical properties of the hadronic system at freeze-out, shown in Table III.

We first observe, comparing the experimental data shown in left hand portion of Table II with the different theoretical results presented on the right hand side, that we are more successful in the description of particles above the horizontal line. Below, in the bottom section of Table II we group results comprising Ω and $\overline{\Omega}$-particles, which seem not to follow the same systematics, a fact already reported with respect of their spectral temperature by the WA97 collaboration [11]. A possible hypothesis is that a good fraction of these particles are made in processes that are different in nature than those leading to the other particle abundances, and hence we excluded Ω and $\overline{\Omega}$-particles from all but one of the approaches presented, denoted F. Moreover, if some strange particles hadronize separately, one cannot demand that the remaining particles balance strangeness exactly and hence we did not in general enforce strangeness conservation, except in case D_s. That case is only slightly worse than D, which implies that the source for both Ω and $\overline{\Omega}$ is nearly symmetric with respect to abundance of strange and anti-strange quarks. This is consistent with the observation that much of the significant asymmetry in the ratio $\overline{\Omega}/\Omega$ arises from the Coulomb effect we described above. We note that model F shown in Table I, including the four Ω-particle data points yields $\chi^2/n_{\mathrm{dof}} = 2.4$ for $n_{\mathrm{dof}} = 8$, the mathematical confidence level is a few percent, it can safely be assumed that our approach is not adequately accounting for the production of Ω-particle.

We address extensively in our study the different constraints, as indicated by the subscript in all tables:

1. D_s includes the requirement of strangeness conservation, *i.e.,* the hadronic phase space has to contain for the given statistical parameters as many $\bar{s}$- as s-quarks. This is most conveniently accomplished by finding the value of λ_s which balances strangeness in terms of the other parameters, and thus, though not fitted, the value shown in Table I displays an error, derived from the errors determined determining the other statistical variables. We note that the phase space occupancies change drastically between cases, D and D_s, see Table I, however the value γ_s/γ_q changes from 0.69 for D to 0.72 for D_s. In actual numerical procedure we took advantage of this stability in γ_s/γ_q-ratio, using it as a parameter. More generally, we note that all acceptable models shown in Table I yield $\gamma_s/\gamma_q = 0.68 \pm 0.05$, which is consistent with the result of model C for γ_s, where the tacit assumption $\gamma_q = 1$ is made.

2. There is considerable reason to seek a comparison of the Pb–Pb system with the analysis of S–Au/W/Pb reactions which we reported earlier [4]. Thus we consider model D_t in which the freeze-out temperature is fixed at the value we found in S–Au/W/Pb reactions, $T_f = 143\,\mathrm{MeV}$. In model D_p, the pressure of the hadron phase space is chosen at the value we found in S–Au/W/Pb reactions, $P = 82\,\mathrm{MeV/fm^3}$. As judged by χ^2/n_{dof} all D_i-models are possible, and the resulting particle multiplicities presented in the columns of Table II differ only in minute detail. The two models D_t and D_p which test consistency with the smaller S–Au/W/Pb reactions are well within the allowable error. This consistency implies the possibility that the matter formed in these two very different systems hadronize in a rather similar fashion, though collective surface flows are very different.

To resolve if there is universal freeze-out we have to consider the physical properties of the fireball. While the statistical parameters shown in Table I can vary strongly from model to model, we find that the implicitly determined physical properties of the hadron source are more stable. In Table III we show for the 8 models along with their temperature the specific energy and entropy content, and specific anti-strangeness content, along with specific strangeness asymmetry, and finally pressure evaluated by using the statistical parameters to characterize the hadronic particle phase space. We note that it is improper in general to refer to these properties as those of a 'hadronic gas' formed in nuclear collisions, as the particles considered may be emitted in sequence, and thus there never is a stage corresponding to a hadron gas phase. However, in the event such a stage exists, we also evaluated (see last column in Table III) the volume of the hadron gas source at chemical decoupling. In order to obtain this extensive property, we used the net baryon number in the fireball being $\langle B - \bar{B}\rangle = 372 \pm 10$, as stated in [10]. Note that a spherical source corresponding to the best model D would have a source radius 9.6 fm, which in turn can be checked to be exactly in agreement with deconfined strangeness conservation as described by Eq. (3), given the statistical parameters, and $m_s \simeq 200\,\mathrm{MeV}$. Other interesting conclusions arising in view of these results and shown in Table III are: the specific energy content E_f/B is well within the expectations based on the collision energy content per nucleon (8.6 GeV) and hence this result confirms firmly the hypothesis that the energy stopping and baryon number stopping in the fireball are very similar [4]. The specific strangeness content of the Pb–Pb collision fireball is, by about 25% smaller than S–Au/W/Pb result [4].

TABLE III

Physical properties of hadronic final state phase space (specific energy, entropy, anti-strangeness, net strangeness, pressure and volume) derived from statistical parameters shown in Table I which describes the Pb–Pb data in Table II. Asterisk * means fixed input.

Fit	$T_{\rm f}$ [MeV]	$E_{\rm f}/B$	$S_{\rm f}/B$	$\bar{s}_{\rm f}/B$	$(\bar{s}_{\rm f}-s_{\rm f})/B$	$P_{\rm f}$ [GeV/fm^3]	$V_{\rm f}$ [fm^3]
A	147 ± 3	6.60 ± 0.40	37.0 ± 3	0.92 ± 0.05	0.29 ± 0.02	0.068 ± 0.005	6429 ± 500
B	142 ± 3	7.13 ± 0.50	40.9 ± 3	1.02 ± 0.05	0.21 ± 0.02	0.053 ± 0.005	8994 ± 600
C	144 ± 4	7.75 ± 0.50	41.7 ± 3	0.70 ± 0.05	0.14 ± 0.02	0.053 ± 0.005	10242 ± 800
D	134 ± 3	8.33 ± 0.50	46.8 ± 3	0.61 ± 0.04	0.08 ± 0.01	0.185 ± 0.012	3619 ± 250
D_s	133 ± 3	8.72 ± 0.50	48.1 ± 3	0.51 ± 0.04	0*	0.687 ± 0.030	1134 ± 100
D_t	143*	7.63 ± 0.45	41.4 ± 3	0.68 ± 0.05	0.12 ± 0.01	0.072 ± 0.005	7517 ± 500
D_p	137 ± 4	8.05 ± 0.50	44.7 ± 3	0.67 ± 0.05	0.13 ± 0.01	0.082*	7090 ± 500
F	334 ± 18	9.79 ± 0.50	24.1 ± 2	0.78 ± 0.05	0.06 ± 0.01	1.64 ± 0.006	2303 ± 250

4. Conclusions

We have presented detailed analysis of hadron abundances observed in central Pb–Pb interactions at 158 A GeV in terms of thermal equilibrium and chemical non-equilibrium phase space model of (strange) hadronic particles. We assumed formation of a thermal dense matter fireball of a priori unknown structure, which explodes and disintegrates into the final state hadrons. We have presented several excellent descriptions of all abundance data which at present comprise 5 or more independent degrees of freedom, yielding a family of models with acceptable confidence level. The physical statistical parameters obtained characterize a strange particle source which, when allowing for Coulomb deformation of the strange and anti-strange quarks, is exactly symmetric, as is natural *only* for a deconfined state. While the statistical parameters shown in table 2 can vary widely there is no way to distinguish with naked eye the different approaches D, D_s, D_t, D_p inspecting the particle abundances shown in Table II. It is important to take note that along with $\lambda_q = 1.62 \pm 0.03, \lambda_s = 1.10 \pm 0.02$ there also is a stable value $\gamma_s/\gamma_q = 0.68 \pm 0.05$ under the different strategies one may follow to analyze the experimental data. The chemical freeze-out temperature allowing for the systematic uncertainty seen in the acceptable group of models in table 2 is $T_\mathrm{f} = 138 \pm 7$ MeV, and this implies that the freeze-out baryochemical potential is $\mu_\mathrm{B} = 199 \pm 3$ MeV. The error here is small, since the best values T_f, λ_q are anti-correlated.

Given these statistical parameters we have also evaluated the physical properties of the hadronic particle phase space, such as energy, entropy and baryon number. The results shown in Table III describe the properties of the final state. These correspond nearly exactly to the initial state conditions, confirming the consistency of our approach and validating the reaction picture applied. This part of our analysis confirms that the reaction proceeds by the way of the formation of a dense fireball comprising highly excited hadronic matter. In consistency with this we obtain values of λ_s which exactly match expectations for strangeness balance in QGP, allowing for the Coulomb effect within the particle source of the size $R_\mathrm{f} = 9.6 \pm 2$ fm. We compare conditions of the particle source for the two systems Pb–Pb and S–Au/W/Pb and find that both can be seen as hadronizing in same physical conditions.

We have compared the lighter system S–Au/W/Pb [4], with the current study of Pb–Pb, selecting comparable freeze-out conditions (models D_t and D_p). We find, see Table III that the different physical properties of the two hadronic source agree. This, along with the strange phase space symmetry and the Coulomb effect, we believe that the sole possible interpretation the formation of a deconfined phase in the initial stages of the collision, which

subsequently evolves and flows apart till it reaches the universal hadronization point, with many similar physical properties, independent of the collision system. System dependent will certainly be the surface collective velocity $\vec{v}_c$ [21], however, our analysis was organized such that this vector field did not enter here in a significant way.

We have begun, using quark-gluon plasma equations of state which incorporate the perturbative corrections and thermal masses, to study detailed scenarios of QGP formation and evolution that leads to the freeze-out properties we obtained here. The important preliminary finding is that it is possible to find QGP-fireballs that naturally lead to the results obtained studying the experimental hadron abundance data, and thus the QGP hypothesis presented here is also consistent with our current theoretical understanding of the QGP equations of state.

We thank E. Quercigh for interesting and stimulating discussions. This work was supported in part by a grant from the U.S. Department of Energy, DE-FG03-95ER40937. LPTHE-Univ. Paris 6 et 7 is: Unité mixte de Recherche du CNRS, UMR7589.

REFERENCES

[1] H. Fritzsch, M. Gell-Mann, H. Leutwyler, *Phys. Lett.* **47 B**, 365 (1973); H.D. Politzer, *Phys. Rep.* **14**, 129-180 (1974) (see p. 154 and Refs [34–41]).

[2] R. Hagedorn, *Suppl. Nuovo Cimento* **2**, 147 (1965); *Cargèse Lectures in Physics*, Vol. 6, Gordon and Breach, New York 1977, and references therein; See also: J. Letessier, H. Gutbrod, J. Rafelski, *Hot Hadronic Matter*, NATO-ASI series B346, Plenum Press, New York 1995.

[3] J. Rafelski, J. Letessier, A. Tounsi, *Acta Phys. Pol.* **B28**, 2841 (1997); *Phys. Lett.* **B410**, 315 (1997).

[4] J. Letessier, J. Rafelski, *Phys. Rev.* **C** in press; [hep-ph/9806386]; submitted to *J. Phys. G* (proceeding of the Padova — Strangeness 1998 conference), [hep-ph/9810332]; J. Rafelski, J. Letessier, A. Tounsi, *Acta Phys. Pol.* **B27**, 1035 (1996), and references therein.

[5] J.W. Harris, B. Müller, *Ann. Rev. Nucl. Part. Sci.* **46**, 71 (1996), and references therein.

[6] J. Rafelski, pp 282–324, GSI Report 81-6, Darmstadt, May 1981; Proceedings of the Workshop on *Future Relativistic Heavy Ion Experiments*, held at GSI, Darmstadt, Germany, October 7–10, 1980, Eds R. Bock and R. Stock, (see in particular section 6, pp 316–320); see also: pp 619–632 in *New Flavor and Hadron Spectrosopy*, Ed. J. Tran Thanh Van, Editions Frontiers 1981, Proceedings of XVIth Rencontre de Moriond — Second Session, Les Arcs, March 21–27, 1981; and: *Nucl. Physics* **A374**, 489c (1982) — Proceedings of ICHEPNC held 6–10 July 1981 in Versailles, France; *Phys. Rep.* **88**, 331 (1982); J. Rafelski, R. Hagedorn, in *Statistical Mechanics of Quarks and Hadrons*, North

Holland, Amsterdam 1981, p. 253; J. Rafelski, M. Danos, *Phys. Lett.* **B192**, 432 (1987).

[7] J. Rafelski, J. Letessier, A. Tounsi, Dallas–ICHEP (1992) p. 983 (QCD161:H51:1992), [hep-ph/9711350];
J. Letessier, A. Tounsi, U. Heinz, J. Sollfrank, J. Rafelski, *Phys. Rev. Lett.* **70**, 3530 (1993); *Phys. Rev.* **D51**, 3408 (1995).

[8] J. Letessier, A. Tounsi, J. Rafelski, *Phys. Rev.* **C50**, 406 (1994); *Acta Phys. Pol.* **A85**, 699 (1994).

[9] F. Pühlhofer, for the NA49 Collaboration, presented at the Tsukuba QM1998 meeting); G.J. Odyniec, *Nucl. Phys.* **A638**, 135 (1998); C. Bormann, for the NA49 Collaboration, *J. Phys. G* **23**, 1817 (1997); G.J. Odyniec, for the NA49 Collaboration, *J. Phys. G* **23**, 1827 (1997); V. Friese for the NA49 Collaboration, *J. Phys. G* **23**, 1837 (1997); D. Röhrig, for the NA49 Collaboration, "Recent results from NA49 experiment on Pb–Pb collisions at 158 GeV per nucleon", here see figure 4, in proceedings of EPS-HEP Conference, Jerusalem, August 19-26, 1997; available at http://www.cern.ch/hep97/abstract/tpa6.htm talk #603; P.G. Jones, for the NA49 Collaboration, *Nucl. Phys.* **A610**, 188c (1996).

[10] F. Becattini, M. Gazdzicki, J. Sollfrank, *Eur. Phys. J.* **C5**, 143 (1998).

[11] E. Andersen *et al.*, WA97-collaboration, *Phys. Lett.* **B433** 209 (1998); K. Safarik *et al.*, WA97-collaboration, *Nucl. Phys* **A630** 582 (1998); A.K. Holme *et al.*, for the WA97 Collaboration, *J. Phys. G* **23**, 1851 (1997).

[12] M. Kaneta *et al.*, NA44-collaboration, *J. Phys. G* **23**, 1865 (1997).

[13] H. Grote, R. Hagedorn, J. Ranft, *Atlas of Particle Production Spectra*, CERN-Service d'Information Scientifique, Geneva 1970.

[14] P. Braun-Munzinger, J. Stachel, J.P. Wessels, N. Xu, *Phys. Lett.* **B365**, 1 (1996).

[15] J. Rafelski, *Phys. Lett.* **B262**, 333 (1991); *Nucl. Phys.* **A544**, 279c (1992).

[16] E. Suhonen, J. Cleymans, K. Redlich, H. Satz, in Proceedings of the International Europhysics Conference on High Energy Physics, Marseille, France, 22-28 July 1993, Marseille EPS HEP 1993, p. 519 (QCD161:I48:1993), [hep-ph/9310345].

[17] U. Heinz, *Nucl. Phys.* **A566**, 205 (1994).

[18] J. Sollfrank, *J. Phys. G* **23**, 1903 (1997), and references therein.

[19] Saeed-Uddin, *J. Phys. G* **24**, 779 (1998).

[20] F. Grassi, O. Socolowski, Jr., *Phys. Rev. Lett.* **80**, 1170 (1998).

[21] J. Letessier, J. Rafelski, Hadronic particle chemical freeze-out with collective flow in 158 A GeV Pb-Pb collisions, in preparation.

[22] J. Rafelski, B. Müller, *Phys. Rev. Lett.* **48**, 1066 (1982); **56**, 2334E (1986); P. Koch, B. Müller, J. Rafelski, *Phys. Rep.* **142**, 167 (1986).

[23] T.S. Biro, J. Zimanyi *Phys. Lett.* **B113**, 6 (1982); *Nucl. Phys.* **A395**, 525 (1983).

[24] B. Müller, J. Rafelski, *Phys. Rev. Lett.* **34**, 349 (1975).